

Cracking the Taub-NUT

Pierre-Philippe Dechant* and Anthony N. Lasenby†

*Astrophysics Group, Cavendish Laboratory,
J J Thomson Avenue, Cambridge, CB3 0HE, UK,
and Kavli Institute for Cosmology, Cambridge*

Michael P. Hobson‡

*Astrophysics Group, Cavendish Laboratory,
J J Thomson Avenue, Cambridge, CB3 0HE, UK*

(Dated: July 17, 2021)

Abstract

We present further analysis of an anisotropic, non-singular early universe model that leads to the viable cosmology presented in [1]. Although this model (the DLH model) contains scalar field matter, it is reminiscent of the Taub-NUT vacuum solution in that it has biaxial Bianchi IX geometry and its evolution exhibits a dimensionality reduction at a quasi-regular singularity that one can identify with the big-bang. We show that the DLH and Taub-NUT metrics are related by a coordinate transformation, in which the DLH time coordinate plays the role of conformal time for Taub-NUT. Since both models continue through the big-bang, the coordinate transformation can become multivalued. In particular, in mapping from DLH to Taub-NUT, the Taub-NUT time can take only positive values. We present explicit maps between the DLH and Taub-NUT models, with and without a scalar field. In the vacuum DLH model, we find a periodic solution expressible in terms of elliptic integrals; this periodicity is broken in a natural manner as a scalar field is gradually introduced to recover the original DLH model. Mapping the vacuum solution over to Taub-NUT coordinates, recovers the standard (non-periodic) Taub-NUT solution in the Taub region, where Taub-NUT time takes positive values, but does not exhibit the two NUT regions known in the standard Taub-NUT solution. Conversely, mapping the complete Taub-NUT solution to the DLH case reveals that the NUT regions correspond to imaginary time and space in DLH coordinates. We show that many of the well-known ‘pathologies’ of the Taub-NUT solution arise because the traditional coordinates are connected by a multivalued transformation to the physically more meaningful DLH coordinates. In particular, the ‘open-to-closed-to-open’ transition and the Taub and NUT regions of the (Lorentzian) Taub-NUT model are replaced by a closed pancaking universe with spacelike homogeneous sections at all times.

PACS numbers: 98.80.Bp , 98.80.Cq , 98.80.Jk , 04.20.Dw , 04.20.Jb , 04.20.dc

Keywords: scalar fields, Bianchi models, big bang singularity, cosmology, exact solutions, Taub-NUT, pre-Big-Bang scenarios

*Electronic address: p.dechant@mrao.cam.ac.uk

†Electronic address: a.n.lasenby@mrao.cam.ac.uk

‡Electronic address: mph@mrao.cam.ac.uk

Contents	
I. Introduction	4
II. Bianchi Models	5
III. The DLH model	7
IV. The Taub-NUT model	9
V. Relationship between DLH and Taub-NUT models	11
VI. The reparameterised Taub-NUT model	13
VII. Comparison of DLH and reparameterised Taub-NUT models	15
A. DLH vacuum solution	15
B. DLH solution with a scalar field	17
C. Taub-NUT vacuum solution	18
1. Mapping the DLH vacuum solution using the diffeomorphism	19
2. Direct solution of Einstein equations for reparameterised Taub-NUT metric	21
3. Comparison of the vacuum solution in different set-ups	22
D. Taub-NUT with a scalar field	26
VIII. Conclusions	30
Acknowledgments	31
A. Mapping of curvature invariants	31
1. Petrov type	32
2. Principal curvatures	33
B. Mapping of geodesics	33
C. Derivation of the elliptic integral solution for the vacuum DLH model	35
References	38

I. INTRODUCTION

In a previous work [1] we argued that it is natural to consider a generalisation of the standard cosmological scenario to one in which a scalar field dominates the dynamics of a homogeneous but, in general, anisotropic (Bianchi) universe. We presented a new solution (the DLH model) to the cosmological field equations based on a closed biaxial Bianchi IX universe containing scalar field matter. This led to a nonsingular ‘pancaking’ model in which the spatial hypersurface volume goes to zero instantaneously at the ‘big-bang’, but all physical quantities, such as curvature invariants and the matter energy density remain finite, and continue smoothly through the big-bang. Moreover, we showed that the model leads to a viable cosmology at late times, exhibiting desirable features such as isotropisation and inflation, as well as producing perturbation spectra consistent with observations.

We also noted in [1] that, despite containing scalar field matter, our model was reminiscent of the Taub-NUT vacuum solution, since both have biaxial Bianchi IX geometry and an evolution that exhibits a dimensionality reduction at a quasi-regular singularity. In this paper, we show that the metrics for the DLH and Taub-NUT models are, in fact, related by a coordinate transformation. It is thus of interest to investigate the explicit mapping between models based on each metric, with and without scalar field matter. Moreover, we investigate the well-known ‘pathologies’ of the Taub-NUT solution, in the context of the mapping to the DLH model. We contend that the natural coordinatisation of the DLH model is more physical than the traditional coordinates used to describe Taub-NUT. We thus consider the possibility that pathologies such as the ‘open-to-closed-to-open’ transition and the Taub and NUT regions of the (Lorentzian) Taub-NUT model arise because the traditional coordinates are connected by a singular transformation to the physically more meaningful DLH coordinates.

This paper is organised as follows. We begin with a description of Bianchi universes in Section II. We then briefly review the DLH model in Section III and the Taub-NUT model in Section IV. We show that the two metrics are related by a coordinate transformation in Section V, where the mapping naturally leads to a new reparameterised form of the Taub-NUT metric. We investigate this reparameterised Taub-NUT model in Section VI and find that it admits a simple scaling family of solutions, in contrast to the conventional Taub-NUT setup. In Section VII, we consider the mapping between the DLH and reparameterised Taub-NUT models, with and without a scalar field, and interpret the solutions physically, before concluding in Section VIII.

II. BIANCHI MODELS

Bianchi universes are spatially homogeneous and therefore have a 3-dimensional group of isometries G_3 acting simply transitively on spacelike hypersurfaces. The standard classification hence follows Bianchi's classification of 3-parameter Lie groups [2].

We adopt the metric convention $(+ - - -)$. Roman letters $a, b, c \dots$ from the beginning of the alphabet denote Lie algebra indices. Greek letters $\mu, \nu, \sigma \dots$ label spacetime indices, whereas Roman letters $i, j, k \dots$ from the middle of the alphabet label purely spatial ones.

The isometry group of a manifold is a Lie group G and can be thought of as infinitesimally generated by the Killing vectors ξ , which obey $[\xi_\mu, \xi_\nu] = C_{\mu\nu}^\sigma \xi_\sigma$ where the $C_{\mu\nu}^\sigma$ are the structure constants of G . These can be used to construct an invariant basis, which is often useful to make the symmetry manifest. This is a set of (basis) vector fields X_μ , each of which is invariant under G , i.e. has vanishing Lie derivative with respect to all the Killing vectors such that

$$[\xi_\mu, X_\nu] = 0. \quad (1)$$

Such a basis can be constructed simply by imposing this relation at a point for some chosen set of independent vector fields and using the Killing vectors to drag them out across the manifold. The integrability condition for this set of first-order differential equations in fact amounts to demanding that the $C_{\mu\nu}^\sigma$ be the structure constants of some group. The invariant vector fields satisfy

$$[X_\mu, X_\nu] = -C_{\mu\nu}^\sigma X_\sigma. \quad (2)$$

Denoting the duals of the X_μ (the so-called invariant 1-forms, or Maurer-Cartan forms) by ω^μ , the corresponding curl relations for the dual basis are

$$d\omega^\mu = \frac{1}{2} C_{\sigma\tau}^\mu \omega^\sigma \wedge \omega^\tau. \quad (3)$$

Because the X_μ are invariant vectors, the metric can now be expressed as

$$ds^2 = g_{\mu\nu} \omega^\mu \omega^\nu, \quad (4)$$

for some $g_{\mu\nu}$.

Bianchi models can be constructed in various different ways. For simplicity, we use the fact that the timelike vector generating the foliation of spacetime into homogeneous spacelike hypersurfaces commutes with the three Killing vectors within the hypersurfaces (generating the homogeneity), and hence we choose a representation that is diagonal:

$$ds^2 = dt^2 - \gamma_{ij}(t) \omega^i \omega^j = dt^2 - \gamma_{kl}(t) (e_i^k(x) dx^i) (e_j^l(x) dx^j), \quad (5)$$

in terms of an explicit (x, y, z) coordinate system.

As outlined in [1], the Bianchi classification of G_3 group types hinges on the decomposition into irreducible parts of the spatial part of the structure constants C^k_{ij} . Imposing the Jacobi identity then essentially leaves nine distinct choices of parameterisations (zeroes and signs) of the structure constants corresponding to nine different groups, called Bianchi I through Bianchi IX. All Bianchi models have a timelike vector, which generates the preferred foliation into spacelike hypersurfaces, and three spacelike Killing vectors, generating the homogeneity on those hypersurfaces. Both models that we will consider, DLH and Taub-NUT, are Bianchi IX such that the symmetry algebra is $\mathfrak{so}(3) \sim \mathfrak{su}(2)$.

General Bianchi IX models are thought, generically, to exhibit complicated dynamics and chaos. The dynamics near the initial singularity of vacuum and orthogonal perfect fluid models is believed to be governed by Bianchi I and II vacuum states via the Kasner map (‘Mixmaster attractor’). This description in terms of successive Kasner periods can be reformulated in terms of reflections and is called ‘cosmological billiard motion’, also known as ‘BKL analysis’ after Belinskii, Khalatnikov and Lifshitz [3–9]. This turns out to be just an example of a more general phenomenon when one considers (super-)gravity close to a spacelike singularity (the ‘BKL-limit’). In this limit the gravitational theory can be recast in terms of billiard motion in a portion of hyperbolic space, as above, such that the dynamics is determined by successive reflections. These reflections, however, are precisely the elements of a Lorentzian Coxeter group, which are themselves the Weyl groups of (infinite-dimensional) Kac-Moody algebras. This then leads to the conjecture that these Kac-Moody algebras are in fact symmetries of the underlying gravitational theory [10–12]. There are also some concerns about the discrete nature of the Kasner map, and a continuous generalisation – see, for instance [13–15]. For recent work on locally rotationally symmetric (LRS) Bianchi cosmologies with anisotropic matter see, for example, [16]. In [1], we remarked on how Bianchi models can be considered as a deformation of Friedmann-Robertson-Walker (FRW) models, and observed how these perturbations freeze out during inflation. In fact, this can be understood in terms of the characterisation of Bianchi IX models as an FRW model deformed by long range gravitational waves [17].

For the DLH and Taub-NUT models that we will consider, however, there exists an additional biaxial symmetry: two of the left-invariant $SU(2)$ one-forms appear with the same coefficient in the metric. Thus there is an additional right action by a $U(1)$ factor inside the $SU(2)$ which acts by isometries, so we are considering a class of metrics admitting an $SU(2) \times U(1)$ symmetry

group. As shown in [1], and demonstrated further below, this additional symmetry allows for much simpler dynamical evolution than in the full triaxial Bianchi IX case.

III. THE DLH MODEL

For the DLH model, the metric of the form (5) is

$$ds^2 = dt^2 - \frac{1}{4}R_1^2(\omega^1)^2 - \frac{1}{4}R_2^2 [(\omega^2)^2 + (\omega^3)^2], \quad (6)$$

which trivially reduces to FRW form in the special case where the two scale factors are equal, $R_1(t) = R_2(t)$. Following [1], and with the usual definitions for the Hubble parameters $H_i(t) \equiv \dot{R}_i/R_i$ for the different directions, the Einstein field equations are easily computed and give two dynamical equations for the two independent radii R_1 and R_2 (from now on we will drop the explicit t dependence of variables):

$$2\dot{H}_2 + 3H_2^2 + \kappa\rho - \Lambda = \frac{1}{R_2^2} \left(3\frac{R_1^2}{R_2^2} - 4 \right) \quad (7)$$

and

$$2H_1^2 + 2\dot{H}_1 - H_2^2 + 2H_1H_2 + \kappa\rho - \Lambda = -\frac{1}{R_2^2} \left(5\frac{R_1^2}{R_2^2} - 4 \right), \quad (8)$$

as well as the Friedmann equation (or Hamiltonian constraint)

$$H_2^2 + 2H_1H_2 - \kappa\rho - \Lambda = \frac{1}{R_2^2} \left(\frac{R_1^2}{R_2^2} - 4 \right), \quad (9)$$

and equation of motion for a simple massive scalar field (for which the potential is given by $V(\phi) = \frac{1}{2}m^2\phi^2$)

$$m^2\phi + (H_1 + 2H_2)\dot{\phi} + \ddot{\phi} = 0. \quad (10)$$

It turns out that these equations have relatively straightforward series solutions in $t - t_0$. We choose $t_0 = 0$ for simplicity, and take it to denote a big bang-like event. In [1] we have presented two solutions with definite parity – one even (bouncing) and one odd (pancaking) in the non-degenerate scale factor R_1 . Here we are interested in the pancaking solution

$$\begin{aligned} R_1(t) &= t (a_0 + a_2t^2 + a_4t^4 + \dots) \\ R_2(t) &= R_3(t) = b_0 + b_2t^2 + b_4t^4 + \dots, \\ \phi(t) &= f_0 + f_2t^2 + f_4t^4 + \dots \end{aligned} \quad (11)$$

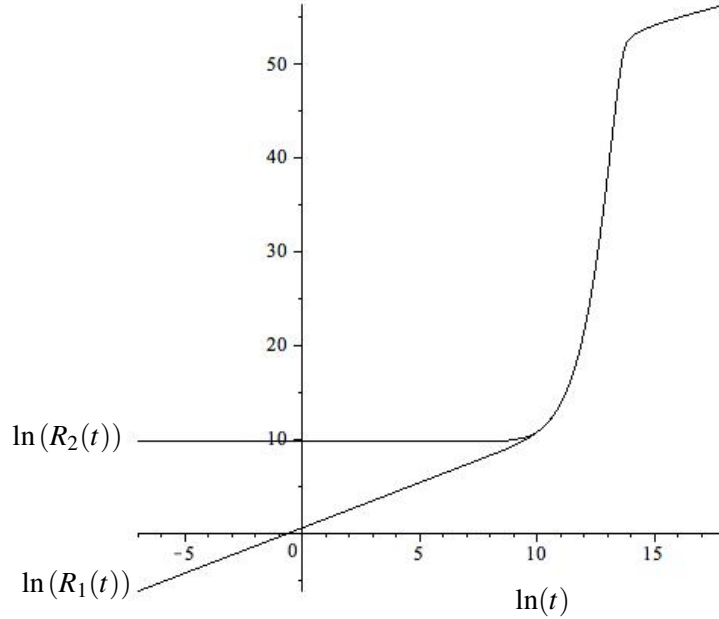


FIG. 1: Dynamics of the DLH biaxial Bianchi IX model: evolution of the logarithm of the scale factors R_1 and R_2 in Planck lengths l_p versus log time (t in units of Planck time t_p).

where the dynamical equations (7), (8) and (10) allow one to fix the higher-order coefficients in the series order-by-order in terms of the initial values $a_0 = \dot{R}_1(0)$, $b_0 = R_2(0)$ and $f_0 = \phi(0)$. The fact that this also satisfies the Friedmann energy constraint (9) then proves that this odd-parity series solution is a valid expansion around the big-bang at $t = 0$, which one can use as a starting point for numerical integration.

Fig. 1 shows the evolution of the scale factors R_1 and R_2 (for $t > 0$) for the viable cosmological solution presented in [1], which is defined by the initial parameters $a_0 = 1.2$, $b_0 = 18000$ and $f_0 = 13$ (set by imposing a boundary condition at temporal infinity on the total elapsed conformal time, as suggested by [18]), together with $\kappa = 1$ and $m = 1/64000$ (set in order to fix the normalisation of the resulting perturbation spectrum) and Λ set to zero, as it is dynamically unimportant at the early time scales that we are interested in. This cosmological model was obtained for a representative set of parameter values of order unity, rather than having been fixed in order to get best agreement with current data. These natural values were then scaled to the seemingly less natural values given above, using a scaling property discussed in the next paragraph. In order to fix the normalisation of the perturbation spectrum, the mass of the scalar field has to be rescaled and b_0 changes to a less natural value accordingly. This choice for the mass of the scalar field needs to be put in by hand for every current inflation model so does not constitute any unusual fine-tuning.

As noted in [1], given a solution to the equations (7)-(10), a family of solutions is generated by scaling with a constant α and defining

$$\bar{R}_i(t) = \frac{1}{\alpha} R_i(\alpha t), \quad \bar{H}_i(t) = \alpha H_i(\alpha t), \quad \bar{\phi}(t) = \phi(\alpha t), \quad \bar{m} = \alpha m, \quad \bar{\Lambda} = \alpha^2 \Lambda. \quad (12)$$

This scaling property is valuable for numerical work, as a range of situations can be covered by a single numerical integration. Furthermore, many physically interesting quantities turn out to be invariant under changes in scale. This scaling property does not, however, survive quantisation, as any quantisation prescription for the scalar field introduces a length scale, which breaks the scale invariance. Therefore one would have to be careful when considering vacuum fluctuations.

In [1] we demonstrated that at the time of pancaking, there is an instantaneous reduction in the number of dimensions of the homogeneous hypersurfaces, without a geometric singularity, or any singularities in physical quantities. Geodesics can extend through this point, though some of them may wind infinitely around the topologically closed dimension. In the light of the generic BKL-analysis mentioned above, it is interesting to note that the dynamics of our model is very straightforward.

IV. THE TAUB-NUT MODEL

The Taub-NUT model [19] is a biaxial Bianchi IX vacuum solution. Traditionally, the form of the metric chosen to describe it does not have the form (5), but is instead written

$$ds^2 = 2du\omega^1 - g(u)(\omega^1)^2 - e^{2\zeta(u)} [(\omega^2)^2 + (\omega^3)^2], \quad (13)$$

where, for later convenience, we denote the standard Ryan & Shepley time coordinate by u (rather than t) and replace their function $\beta(t)$ by $\zeta(u)$.

The metric (13) can be shown to solve the vacuum Einstein equations provided

$$g(u) = \frac{Au + 1 - 4B^2u^2}{B(4B^2u^2 + 1)}, \quad e^{\zeta(u)} = \left(Bu^2 + \frac{1}{4B} \right)^{\frac{1}{2}}, \quad (14)$$

where A and B are arbitrary constants, which when varied lead to a family of solutions. The above functions are plotted in Fig. 2 for the choice of values $A = B = 1$. Note that $e^{\zeta(u)}$ is always positive as asserted in [19], but also that it behaves like $|u|$ for large values of B or u , whereas $g(u)$ has the form of an inverted parabola for small u and approaches a constant for large u . Essentially, B measures the smoothness of $e^{\zeta(u)}$ at the origin, whereas A shifts the centre of the approximate

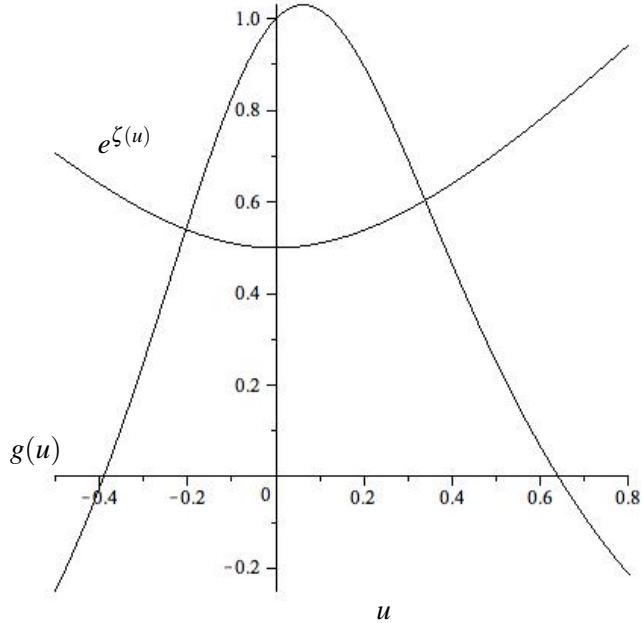


FIG. 2: Analytic Taub-NUT solution (14) for $A = B = 1$.

parabola $g(u)$. We note that there is no analogue of the simple scaling family of solutions (12) in this setup.

The usual interpretation of Fig. 2 is that Taub-NUT has two NUT regions, corresponding to negative values of g and one Taub region, where g is positive. One infers that the Taub-NUT solution can be represented as a disc that evolves into an ellipsoid and back into a disc. In particular, it is considered to evolve from timelike open sections in a NUT region, via lightlike sections (called Misner bridges), to spacelike closed sections in the Taub region, back into timelike open sections in the other NUT region. This open-to-closed-to-open transition is not mathematically singular, but it is incomplete, as geodesics spiral infinitely many times around the topologically closed spatial dimension as they approach the boundary [20–26] (see, for instance, [27] for a recent treatment). This type of singularity is called ‘quasiregular’ in the Ellis and Schmidt classification [28, 29] (these include the well-known ‘conical’ singularities [30]), as opposed to a (scalar or non-scalar) curvature singularity. The Taub-NUT solution therefore shows the same feature of dimensional reduction as the DLH model and similarly does not have a geometric singularity during this collapse. Note, however, that the homogeneous hypersurfaces are only spacelike in the Taub region, leading to problems with Taub-NUT as a description of a homogeneous universe as one approaches the boundaries of the Taub region (the Misner bridges).

V. RELATIONSHIP BETWEEN DLH AND TAUB-NUT MODELS

The similarities between the DLH and Taub-NUT models are sufficiently striking that the connection between the two models warrants further consideration. In particular, it is known that Taub-NUT is the only Petrov type D homogeneous closed vacuum spacetime and that all Petrov D solutions are known [31]. It is a straightforward, if tedious, calculation to show that the DLH metric (6) is also of Petrov type D. Moreover, one finds that the DLH and Taub-NUT metrics have the same degeneracy structure in their principal curvatures, i.e. the eigenvalues of the Riemann tensor (rather than the Weyl tensor used in the Petrov classification), in that there are two degenerate pairs and two singlets amongst the six real eigenvalues, as further explained in appendix A. Furthermore, the most general biaxial Bianchi IX metric is also known to be the Plebański-Demiański metric [32]. The similar behaviour of geodesics in both models is also suggestive. An analysis of geodesics in both models is contained in appendix B, and more details can be found in [1]. These similarities suggest that the DLH and Taub-NUT metrics might describe the same spacetime geometry. In fact, as we now demonstrate, the two metrics are indeed related by a coordinate transformation.

In general, the diffeomorphism invariance of general relativity means it can be difficult to determine if two metrics describe genuinely different spacetime geometries or are the same up to a diffeomorphism. Nonetheless, in the latter case, such a diffeomorphism can be found from considering several scalar invariants. In general, four independent scalar invariants allow us to fix the diffeomorphism between the two spacetimes. A further invariant can then be used to check consistency or to derive a contradiction. In our present case, both models are homogeneous and so scalar invariants are functions of time only. Thus, by considering how a single curvature invariant, e.g. the Ricci scalar, transforms, one can straightforwardly identify an appropriate coordinate transformation linking the two metrics, which amounts simply to a time rescaling.

Starting with the DLH metric (6), let us consider the time rescaling transformation

$$u = \int_0^t \frac{1}{2} R_1(t') dt' \equiv f^{-1}(t) \quad (15)$$

and define the functions $P_i(u) \equiv R_i(f(u)) = R_i(t)$. The lower limit on the integral is chosen for convenience such that $u = 0$ when $t = 0$. One could make another choice, but this simply adds a constant shift to the value of u . Moreover, let us shift the non-degenerate spatial one-form by a

timelike part to obtain

$$\sigma^1 \equiv \omega^1 + \frac{2}{R_1(t)} dt, \quad \sigma^2 \equiv \omega^2, \quad \sigma^3 \equiv \omega^3. \quad (16)$$

The shift is necessary to absorb unwanted terms arising from the time reparameterisation into a redefinition of the one-forms. As long as the one-forms are purely spatial to start with, the timelike component that we have added to the first one-form commutes through, such that this redefined set of one-forms still obeys the $\mathfrak{su}(2)$ commutation relations and is therefore a valid set to describe homogeneous hypersurfaces. One thus obtains the metric

$$ds^2 = 2du\sigma^1 - \frac{1}{4}P_1(u)^2(\sigma^1)^2 - \frac{1}{4}P_2(u)^2 [(\sigma^2)^2 + (\sigma^3)^2]. \quad (17)$$

Comparing this expression with the Taub-NUT metric (13), one sees that they have the same form, but with $\frac{1}{4}P_1^2$ replacing g and $\frac{1}{4}P_2^2$ replacing $e^{2\zeta}$. It is straightforward to verify that the time rescaling (15) maps all curvature scalars for the DLH metric, such as the Ricci scalar (by construction), the Euler-Gauss-Bonnet invariant

$$R_{GB}^2 = R_{\mu\nu\sigma\tau}^2 - 4R_{\mu\nu}^2 + R^2, \quad (18)$$

the Chern-Pontryagin scalar

$$K_{CP} = {}^*R_{\mu\nu\sigma\tau}R^{\mu\nu\sigma\tau}, \quad (19)$$

and the eigenvalues of the Riemann and Weyl tensors (of course they are not necessarily independent) into those obtained for the Taub-NUT metric (c.f. appendix A). Moreover, we note that the form of the resulting Einstein field equations do not depend on the concrete realisation of the $\mathfrak{su}(2)$ 1-forms used in the metric; one simply requires that they obey the $\mathfrak{su}(2)$ algebra commutation relations, which we have guaranteed by construction. A mapping between the geodesic equations in both models, for the explicit realisation used in [1], is exhibited in appendix B.

The time rescaling transformation (15) is valid independently of any concrete choice for the metric functions. Nonetheless, it can be seen that whenever $R_1(t)$ (or $P_1(u)$) goes through zero, as is the case at pancaking events of the DLH model (or on the Misner bridges in the Taub-NUT model), this coordinate transformation will be problematic. The transformation itself is not singular, but one sees that when the integrand R_1 changes sign (such as at the pancaking events), the definition of u becomes multivalued: the value of the integral for u will begin to decrease as t increases. Thus there is only a one-to-one correspondence between u and t as long as R_1 and P_1

do not change sign. Furthermore, the definition of the 1-forms (16) goes singular at the pancaking events also indicating a problem with u as a measure of time (c.f. Section VII D).

We also note that from (15) we have that

$$\frac{du}{dt} = \frac{R_1(t)}{2} = \frac{P_1(u)}{2}, \quad (20)$$

and thus the inverse transformation is simply given by

$$t = \int_0^u \frac{2}{P_1(u')} du'; \quad (21)$$

Hence DLH time t is essentially conformal time for Taub-NUT. This seems rather odd, as DLH is the natural generalisation of closed FRW models, and one is usually interested in conformal time associated with those cosmologically interesting solutions, which would make the usual cosmological conformal time doubly conformal Taub-NUT time.

VI. THE REPARAMETERISED TAUB-NUT MODEL

The new form (17) for the Taub-NUT metric differs significantly from the traditional form (13). We believe that our new form in terms of the scale factors is physically more meaningful, as the squares of the scale factors premultiply the invariant one-forms, as in the DLH metric, or in the FRW special case, to give physical distances on the homogeneous spacelike slices.

The differences between our form (17) and the traditional form (13) brings into question the usual interpretation of the Taub-NUT vacuum solution (14). In particular, we see that the traditional g function is rather unnatural, as it corresponds to the square of a scale factor, rather than the more physically meaningful scale factor itself. Moreover, as the square of a real number, the function g should always be positive. Hence we should not allow the g function to go negative, and must instead select the positive branch at all times. This yields a very different picture from the alleged open-to-closed-to-open transition. If one simply took the modulus of the solution in Fig. 2, such that the g -function is positive throughout, the resulting model is not a solution of the Einstein equations, unless $e^{2\zeta}$ is also allowed to flip sign and become negative, thus raising a new problem. Rather, one should solve afresh the Einstein equations using the reparameterised Taub-NUT metric as the Ansatz.

In our parametrisation (17), in terms of the scale factors $P_i(u)$, with associated Hubble functions $K_i(u) \equiv P_i'/P_i$ (where a prime denotes d/du) and scalar field $F(u) \equiv \phi(f(u)) = \phi(t)$, the Einstein

field equations yield the dynamical equations

$$4P_1^2 K_1' + 8P_1^2 K_1^2 - 2P_1^2 K_2^2 - 4\kappa m^2 F^2 + \kappa P_1^2 F'^2 + 4P_1^2 K_1 K_2 - 8\Lambda + \frac{8}{P_2^2} \left(5 \frac{P_1^2}{P_2^2} - 4 \right) = 0 \quad (22)$$

and

$$4P_1^2 K_2' + 6P_1^2 K_2^2 - 4\kappa m^2 F^2 + \kappa P_1^2 F'^2 + 4P_1^2 K_1 K_2 - 8\Lambda - \frac{8}{P_2^2} \left(3 \frac{P_1^2}{P_2^2} - 4 \right) = 0, \quad (23)$$

as well as the Friedmann equation (or Hamiltonian constraint)

$$-2P_1^2 K_2^2 + 4\kappa m^2 F^2 + \kappa P_1^2 F'^2 - 4P_1^2 K_1 K_2 + 8\Lambda + \frac{8}{P_2^2} \left(\frac{P_1^2}{P_2^2} - 4 \right) = 0, \quad (24)$$

and, in general, the equation of motion for the scalar field

$$P_1^2 F'' + 2P_1^2 (K_1 + K_2) F' + 4m^2 F = 0. \quad (25)$$

It is straightforward to show that, as expected, these equations also result from directly applying the time rescaling transformation (15) and associated function redefinitions to the evolution equations (7)-(10) of the DLH model.

We will solve the above system of equations, with and without scalar matter, in Section VII. For the moment, however, we concentrate on the issue of scaling solutions. Considering the family of solutions in the DLH model related by (12), one could use the time rescaling transformation (15) to map these solutions into our reparameterised Taub-NUT model, thereby constructing an analogous family of Taub-NUT solutions. In general, however, these will not be related by a simple scaling relation as in (12). Nonetheless, our reparameterised version of Taub-NUT does admit directly a family of solutions that are related by a straightforward scaling of the form

$$\bar{P}_i(u) = \frac{1}{\sqrt{\beta}} P_i(\beta u), \quad \bar{K}_i(u) = \beta K_i(\beta u), \quad \bar{F}(u) = F(\beta u), \quad \bar{m} = \sqrt{\beta} m, \quad \bar{\Lambda} = \beta \Lambda. \quad (26)$$

Comparing this result with the corresponding scaling invariance (12) of solutions in the DLH model, we see that they both arise from a simple constant time rescaling of the form $t \rightarrow \alpha \bar{t}$ (in the DLH model) or $u \rightarrow \beta \bar{u}$ (in the reparameterised Taub-NUT model). The relative square root between α and β results from the fact that the Taub-NUT metric is linear in the ‘time’ parameter u whereas the DLH metric is quadratic in t .

The integral definition (15) of $u(t)$ precludes a straightforward identification of $u(\alpha t)$ with $\alpha u(t)$. One can, however, extend the diffeomorphism (15) to take us from scaled DLH to scaled Taub-NUT by writing

$$\beta \bar{u} = \int_0^{\alpha \bar{t}} \frac{1}{2} R_1(t') dt' \quad (27)$$

and

$$\sigma^1 \equiv \omega^1 + \frac{2\alpha}{R_1(\alpha\bar{t})}d\bar{t}, \quad \sigma^2 \equiv \omega^2, \quad \sigma^3 \equiv \omega^3, \quad (28)$$

and defining $P_i(\beta\bar{u}) \equiv R_i(\alpha\bar{t})$ and $F(\beta\bar{u}) = \phi(\alpha\bar{t})$.

VII. COMPARISON OF DLH AND REPARAMETERISED TAUB-NUT MODELS

Although there exists a coordinate transformation linking the DLH and reparameterised Taub-NUT metrics, this transformation is multivalued when pancaking events occur in the DLH model and at the Misner bridges in the Taub-NUT model; this leads to differences in the physical interpretation of the corresponding cosmological solutions. In this section, we therefore consider, in turn, the four cases of vacuum and scalar field matter solutions in both DLH and reparameterised Taub-NUT. We contend that the DLH set-up is the more physically meaningful. Anticipating this conclusion, we start by considering the DLH vacuum model as the most fundamental setup.

A. DLH vacuum solution

Setting the scalar field $\phi = 0$ in the DLH evolution equations (7)-(10), and also assuming $\Lambda = 0$ for simplicity, as it is unimportant dynamically at early times, yields the system

$$2\dot{H}_2 + 3H_2^2 = \frac{1}{R_2^2} \left(3\frac{R_1^2}{R_2^2} - 4 \right), \quad (29)$$

$$2H_1^2 + 2\dot{H}_1 - H_2^2 + 2H_1H_2 = -\frac{1}{R_2^2} \left(5\frac{R_1^2}{R_2^2} - 4 \right), \quad (30)$$

$$H_2^2 + 2H_1H_2 = \frac{1}{R_2^2} \left(\frac{R_1^2}{R_2^2} - 4 \right), \quad (31)$$

which can be solved analytically, albeit in terms of elliptic integrals. The detailed derivation of the analytic form is given in appendix C. In short, the Einstein equations can be integrated to find one scale factor R_1 and time t in terms of the other scale factor R_2 as

$$R_1(t) = \pm \frac{R_2(t)\dot{R}_2(t)}{\sqrt{\mu R_2(t)^2 - 1}}, \quad (32)$$

and

$$t = \sqrt{\frac{i}{2a_0} \frac{x^2 + a_0^2}{a_0^2 + 4}} y + \sqrt{\frac{a_0}{8i}} E(y; i) + \sqrt{\frac{ia_0}{32}} (a_0 + 2i) F(y; i) - \sqrt{\frac{i}{32a_0}} (a_0^2 - 4) \Pi\left(y; \frac{2}{ia_0}; i\right), \quad (33)$$

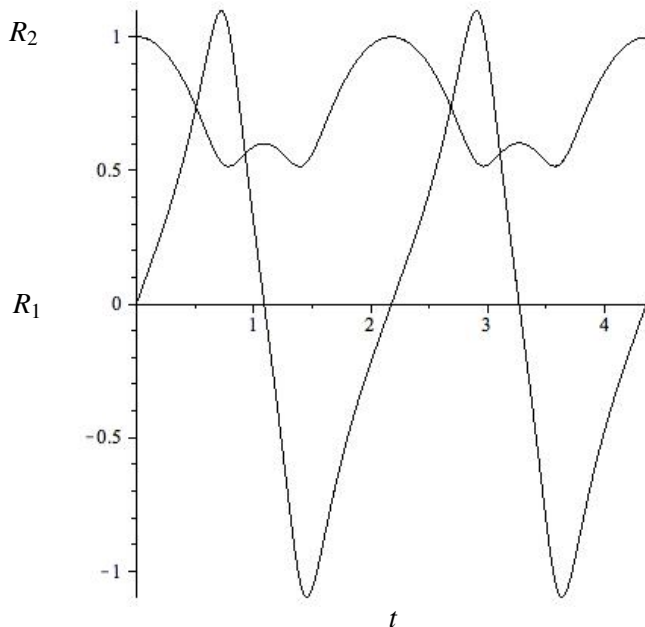


FIG. 3: Periodic ‘DLH vacuum’ solution for the values $a_0 = 1$ and $b_0 = 1$.

where $E(z; k)$, $F(z; k)$ and $\Pi(z; v; k)$ are Legendre’s three normal forms, μ an integration constant that can be fixed in terms of the initial conditions, and x and y are functions of R_2 defined in appendix C. Alternatively, the system of evolution equations can be solved numerically; comparison of the numerical and analytical solutions shows very good agreement (see Fig. 15).

The solution is periodic in t , as shown in Fig. 3, which is a numerical solution with boundary conditions analogous to the pancaking solution in the case with the scalar field (11), i.e.

$$R_1(0) = 0, \dot{R}_1(0) = a_0, R_2(0) = b_0, \dot{R}_2(0) = 0, \quad (34)$$

and we make the convenient choice $a_0 = 1$, $b_0 = 1$. In addition to the periodicity, the solution is symmetric about the two pancaking points in each period, with a parity inversion in R_1 (which is linear near pancaking events) and R_2 being even, in agreement with our previous pancaking DLH solution in [1]. This is an interesting ‘cyclic’ model that repeats indefinitely. As we will see in the following section, it is stable to inclusion of a perturbing scalar field, but as the scalar field becomes heavier and/or denser, strict periodicity is broken.

B. DLH solution with a scalar field

This physical set-up is, of course, that which we originally considered in [1]. As re-iterated in Section III, for some (quite natural) assumed values of the initial conditions and scalar field mass, such a model leads to a viable cosmology. It is of interest here, however, to investigate the transition from the cyclic DLH vacuum solution outlined above to the viable cosmological model by ‘gradually’ introducing the scalar field. This can be achieved by allowing the scalar field to become progressively denser or the mass of the scalar field heavier. Here the same boundary conditions are assumed as previously for the pancaking series solution (11), i.e. oddness for R_1 and evenness for R_2 and ϕ .

In order to assess the effect of increasing scalar field energy density, the remaining parameters are kept constant at $\kappa = 1$, $\Lambda = 0$, $m = 1/64000$, $a_0 = 1$, $b_0 = 1$, whilst ϕ_0 is varied over the range $0 \leq \phi_0 \leq 2 \times 10^5$. Fig. 4 shows the vacuum solution in panel (a), and a small perturbation thereof, with $\phi_0 = 4$, in panel (b). As the scalar field is increased, R_1 turns around (panel c) and inflation is produced (panel d) (both for $\phi_0 = 1.22 \times 10^5$). Note that, from panel (d) onwards, we increase the range in t and take logarithms of the scale factors, to account for the fact that inflation is produced. Panels (e) and (f) show how higher initial scalar field energy densities produce more inflation (for $\phi_0 = 1.3 \times 10^5$ and $\phi_0 = 2.0 \times 10^5$ respectively).

Similarly, in order to study the effects of increasing the mass of the scalar field (Fig. 5) (rather than its density), the other parameters are kept fixed at $\kappa = 1$, $\Lambda = 0$, $\phi_0 = 1.0$, $a_0 = 1$, $b_0 = 1$, whilst m takes the values: (a) $m = 1$, (b) $m = 3$, (c) $m = 5$, (d) $m = 10$ and (e) $m = 100$. Panel (f) shows the $m = 100$ case for a wider range in t .

For a very light or diffuse scalar field, the equation of motion

$$m^2 \phi + (H_1 + 2H_2) \dot{\phi} + \ddot{\phi} = 0 \quad (35)$$

is approximately satisfied by a constant scalar field, as the mass term is suppressed. This essentially eliminates the scalar field from the problem, so that we recover the vacuum case with its periodic behaviour. As the scalar field gets denser (see Fig. 4) or the mass of the scalar field heavier (see Fig. 5) (but still subject to the same boundary conditions), the deviations from the vacuum case grow, and eventually can no longer be considered small. The behaviour is then no longer periodic, and smoothly changes qualitatively, eventually yielding the inflationary cosmological solution described in [1].

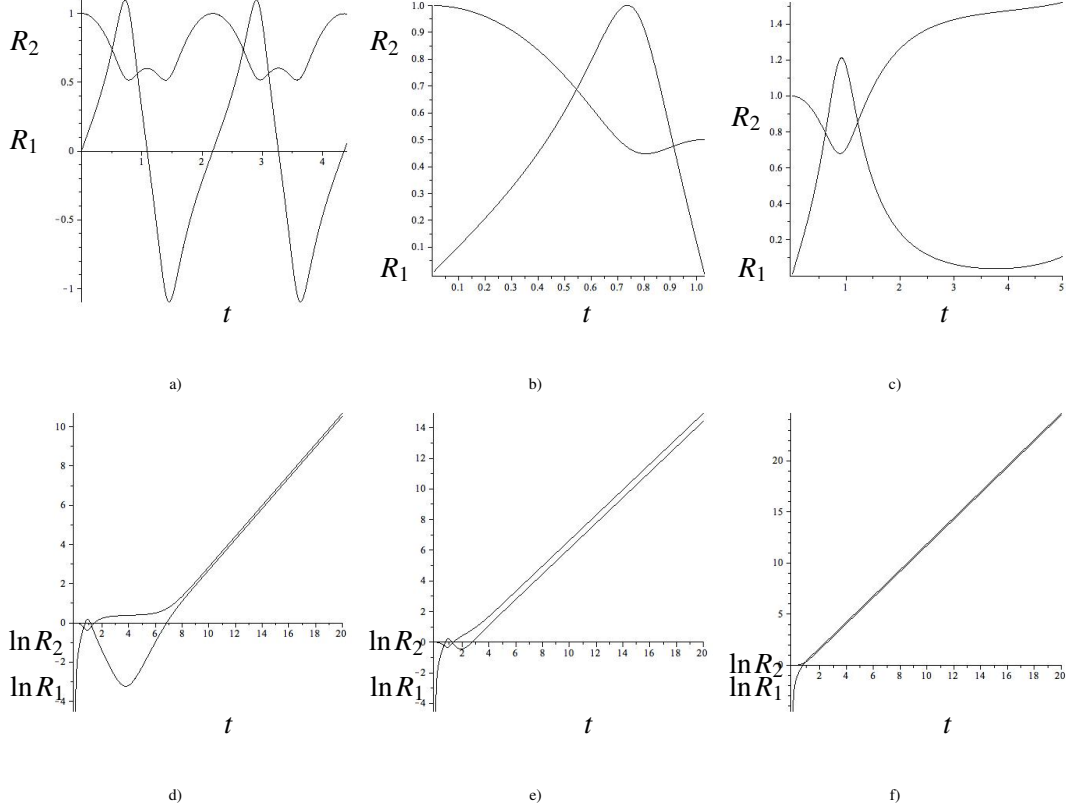


FIG. 4: Gradually introducing a light scalar field by increasing ϕ_0 , whilst keeping the other parameters fixed at $\kappa = 1$, $\Lambda = 0$, $m = 1/64000$, $a_0 = 1$, $b_0 = 1$: a) shows the vacuum model $\phi_0 = 0$; b) $\phi_0 = 4$; c) and d) both have $\phi_0 = 1.22 \times 10^5$; e) $\phi_0 = 1.3 \times 10^5$ and (f) $\phi_0 = 2 \times 10^5$.

C. Taub-NUT vacuum solution

The usual derivation of the Taub-NUT vacuum solution is obtained by substituting the standard form of the metric (13) into the Einstein equations to yield the family of solutions (14). We now have two further methods for constructing this solution: by mapping the DLH vacuum solution using the diffeomorphism (15); and by substituting our reparameterised form (17) of the Taub-NUT metric into the Einstein equations and solving the resulting system of equations given in Section VI. These two alternative approaches offer different physical insights into the nature of the Taub-NUT vacuum solution, and are considered below.

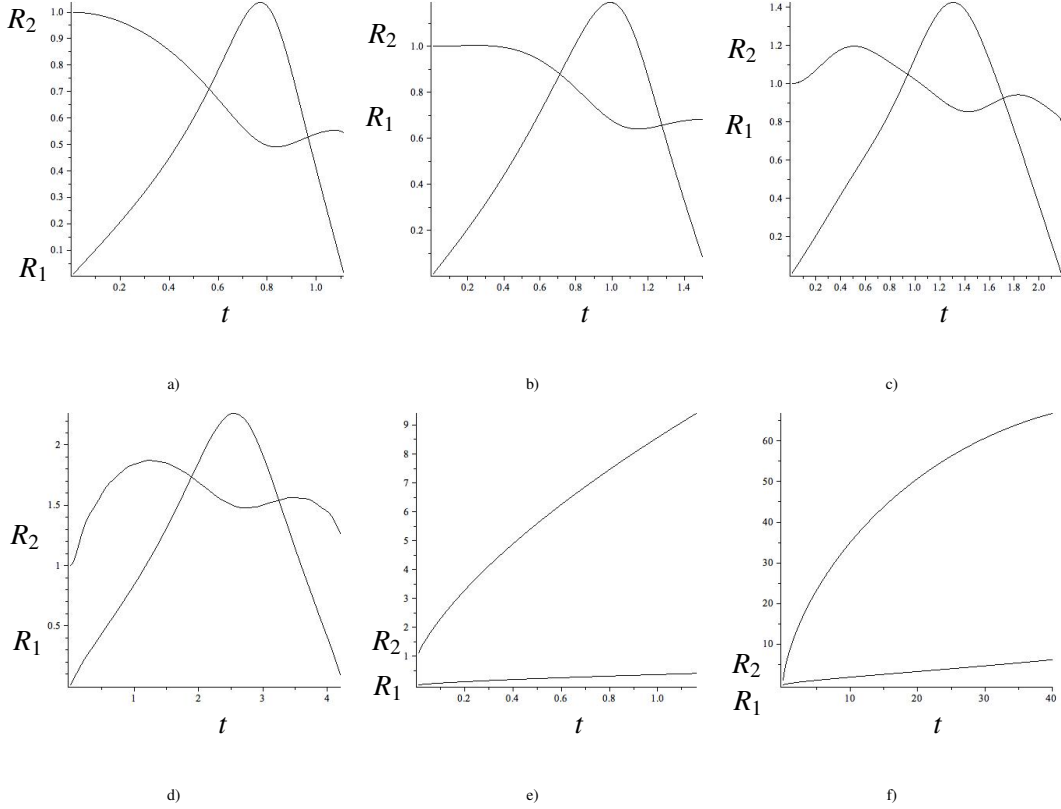


FIG. 5: Gradually increasing the mass of the scalar field whilst keeping the other parameters fixed at $\kappa = 1$, $\Lambda = 0$, $\phi_0 = 1$, $a_0 = 1$, $b_0 = 1$: (a) shows the model for $m = 1$; (b) $m = 3$; (c) $m = 5$; (d) $m = 10$; (e) and (f) are both for $m = 100$, with the latter covering a wider range in t .

1. Mapping the DLH vacuum solution using the diffeomorphism

Conceptually, the simplest way to arrive at the vacuum solution for the reparameterised Taub-NUT metric is to apply the diffeomorphism (15) to the DLH vacuum solution discussed in Section VII A. In practice, however, this is rather complicated, as it involves elliptic integrals. For the sake of simplicity, we therefore concentrate on the period near (one of) the pancaking events, which will be sufficient to unearth some interesting properties of the mapping.

In the vicinity of a pancaking event, R_1 has the simple linear behaviour

$$R_1(t) = a_0 t. \quad (36)$$

Hence, the corresponding coefficient in the DLH metric (6), which is proportional to $R_1^2 \propto t^2$, is a smooth function that touches zero at the pancaking (see Fig. 6). To map this solution to the reparameterised Taub-NUT model, we first use the definition of u in the diffeomorphism (15) to

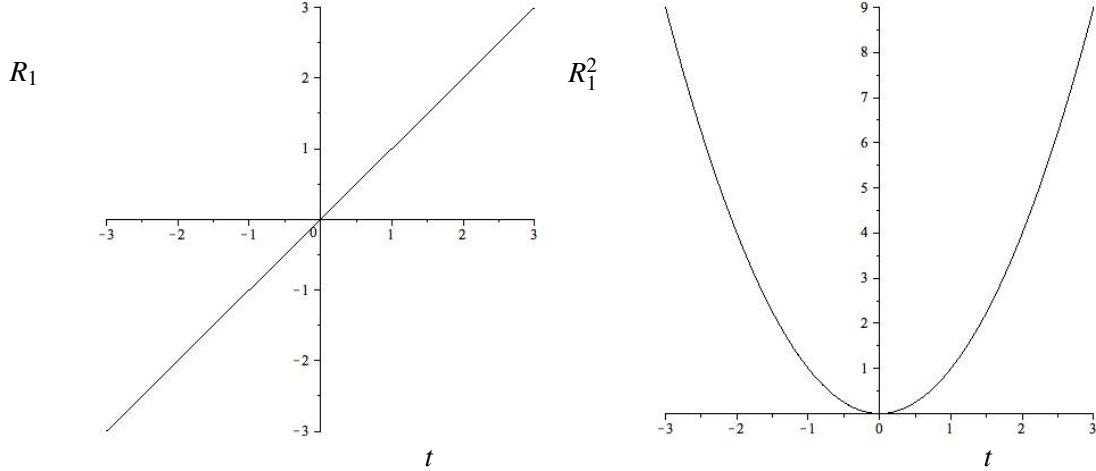


FIG. 6: Near-pancake limit of the DLH solution: $R_1(t)$ and $R_1^2(t)$

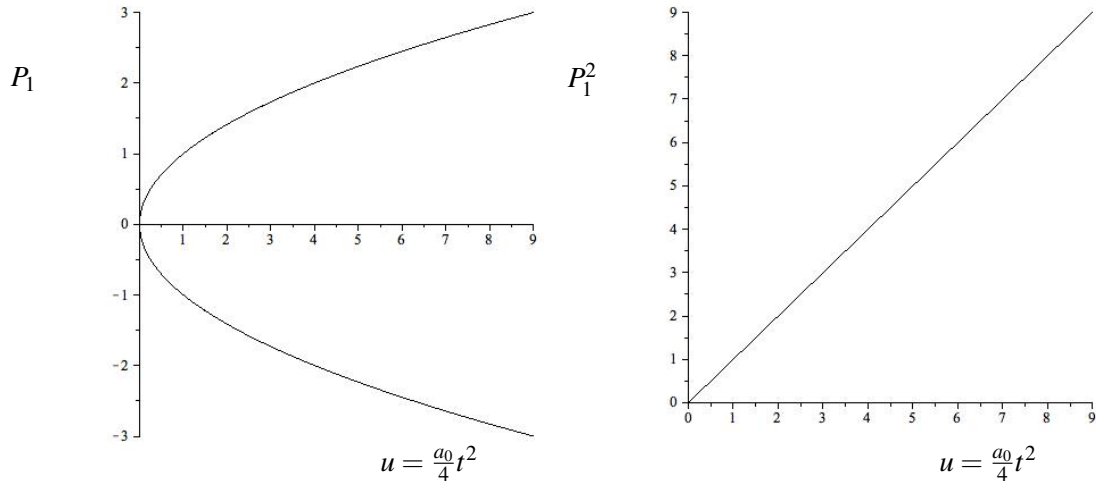


FIG. 7: Near-pancake limit of the Taub-NUT solution: $P_1(u)$ and $P_1^2(u)$

obtain

$$u = \int_0^t \frac{1}{2} a_0 t' dt' = \frac{1}{4} a_0 t^2, \quad (37)$$

in this limit. Thus u is always positive (assuming $a_0 > 0$), whilst t takes both positive and negative values. Also, since $R_1(t) = P_1(u)$, this yields

$$P_1^2(u) = a_0^2 t^2 = 4a_0 u. \quad (38)$$

We see immediately that the innocuous pancaking of the DLH solution now appears as $\pm\sqrt{u}$ behaviour in the corresponding Taub-NUT solution (see Fig. 7); this also matches the lowest order term in a series expansion of a solution to the Taub-NUT Einstein field equations (22)-(25). From the multivaluedness, we see that u is ill-defined as a time variable, as we cannot access negative

values of u here, whereas $P_1(u)$ is multivalued as a function of u . Even more pathologically, P_1^2 (which essentially plays the same role as $g(u)$) seems to originate only at $u = 0$, and then extend out to infinity in a straight line. In terms of the description in terms of time t , P_1^2 comes in from infinity, reaches the origin, and then traces back on itself. This already hints at an observation that will be made more precise below: our inability to access negative values of u presumably amounts to those values corresponding to some Euclidean, imaginary time coordinate obtained by a Wick rotation from the physical time t . Of course, the behaviour described here depends on the exact choice of the lower limit of the integration in the definition of u , but making a different choice does not avert the problem; it simply adds a constant offset to u .

2. Direct solution of Einstein equations for reparameterised Taub-NUT metric

Setting the scalar field $F = 0$ (and $\Lambda = 0$) in (22)-(24), we can, in complete analogy with Section VII A, solve directly for the Taub-NUT model parameterised in terms of P_1 and P_2 . Note that we have already shown that for this coordinatisation there exists a simple scaling solution (26), contrary to the original Ryan-Shepley form (14).

The vacuum equations

$$4K_1' + 8K_1^2 - 2K_2^2 + 4K_1K_2 + \frac{8}{P_1^2P_2^2} \left(5\frac{P_1^2}{P_2^2} - 4 \right) = 0, \quad (39)$$

$$4K_2' + 6K_2^2 + 4K_1K_2 - \frac{8}{P_1^2P_2^2} \left(3\frac{P_1^2}{P_2^2} - 4 \right) = 0, \quad (40)$$

$$-2K_2^2 - 4K_1K_2 + \frac{8}{P_1^2P_2^2} \left(\frac{P_1^2}{P_2^2} - 4 \right) = 0, \quad (41)$$

can be immediately integrated by again taking an appropriate combination of a dynamical equation and the Friedmann equation to give

$$P_2(u) = \left(\frac{1 + \mu^2(u + u_0)^2}{\mu} \right)^{\frac{1}{2}}, \quad (42)$$

where μ is a constant of integration. Note that $P_2(u)$ never goes to zero. In fact this form for $P_2(u)$ is nearly identical to the square-root of the standard form for $g(u)$ in the Taub-NUT solution given in (14). The slight difference occurs because our time coordinate u differs to the one used by Ryan & Shepley, in general, by a relative shift u_0 . In (14), u_0 was chosen to be zero such that the function was symmetric around $u = 0$. Here, we will instead enforce our usual boundary

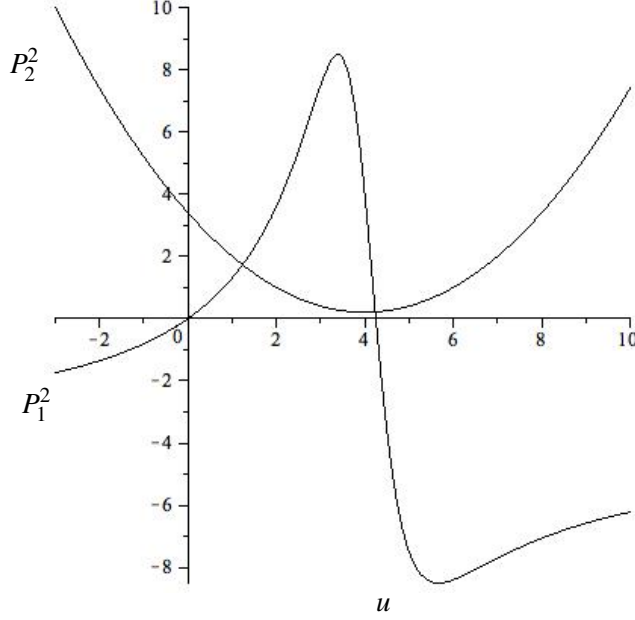


FIG. 8: Analytic Taub-NUT solution in terms of P_1 and P_2 for $\mu = \beta = 1$.

conditions on P_1 , namely that it passes through zero when $u = 0$, with a certain slope. Substituting the expression for P_2 into the Friedmann constraint allows us to integrate to find P_1^2 , with some additional integration constant β . Now choosing $u_0 = -\frac{4}{\beta\mu}$ such that P_1 vanishes at $u = 0$, we find

$$P_1^2(u) = \left(\frac{\beta u(-4\beta\mu u + \beta^2 + 16)}{\beta^2\mu^2 u^2 - 8\beta\mu u + \beta^2 + 16} \right). \quad (43)$$

$$P_2^2(u) = \left(\frac{\beta^2\mu^2 u^2 - 8\beta\mu u + \beta^2 + 16}{\mu\beta^2} \right), \quad (44)$$

Note the similarity with the derivation in Section VII A. We could now eliminate the integration constants in favour of a_0 and b_0 , or rather their equivalent series initial conditions. The functions $P_1(u)$ and $P_2(u)$ are plotted for $\mu = \beta = 1$ in Fig. 8.

3. Comparison of the vacuum solution in different set-ups

It is clear from comparing (13) with (17) that g and P_1^2 are in correspondence

$$\frac{1}{2}P_1^2(u) \sim g(u), \quad (45)$$

and that the degenerate radii are straightforwardly related as

$$\frac{1}{2}P_2(u) \sim e^{\zeta(u)}, \quad (46)$$

where the \sim is taken to denote equivalence up to the above shift u_0 .

One sees that applying the above identifications (46) and (45) to the Taub-NUT scaling family (26), one obtains a family of solutions even in the conventional setup:

$$\bar{g}(u) = \frac{1}{\sqrt{\beta}}g(\beta u), \quad \bar{\zeta}(u) = \zeta(\beta u) - \frac{1}{2}\ln\beta. \quad (47)$$

This can also be seen from changing the time parameter in the metric itself as before. However, this transform looks less natural than the one for DLH, adding to the suspicion that Taub-NUT time is not a physically sensible coordinate.

One may continue to match the vacuum solution in the three different set-ups analytically. The above matching of the radii in the two versions of Taub-NUT together with the relative time shift u_0 allow one to identify A and B in terms of μ and β . This now completes the identification of the two Taub-NUT versions. These two equivalent models can now in turn be related to the initial conditions a_0 and b_0 in the (original and periodic) DLH model using the time reparameterisation (15).

In fact, all three models can be shown to coincide, at least for the portion where the radius in Taub-NUT corresponds to some physical distance ($g(u) \sim P_1^2(u) > 0$), i.e. where taking the square root gives something real. Fig. 9 displays $\sqrt{g} \sim P_1$ from their analytical forms (14) and (43) in the range where $g(u) \sim P_1^2 > 0$ (\sqrt{g} dashed, P_1 dotted). They are found to be in agreement with our matching of these two solutions analytically above. Furthermore, they also coincide with a plot of $R_1(t) = P_1(u)$ as a function of $u(t)$ as defined by (15), evaluated for the periodic DLH vacuum solution considered above. However, whereas \sqrt{g} and P_1 only live in the upper half plane, the mapped DLH solution winds around a mirror-symmetric closed parametric curve in P_1 - $u(t)$ -space as it cycles through its periodic oscillations, with one half-period of the elliptic solution corresponding to the positive portion of g . The other radii e^ζ , P_2 and R_2 match likewise.

This now raises the question: to what do the parts of the analytic Taub-NUT solutions with $g < 0$ correspond when mapped over to the DLH setup using the inverse mapping (21)? Clearly, in this regime, the physical radius $P_1 = R_1$ must become imaginary. The prescription for finding $t(u)$ then indicates that time t must likewise become imaginary, as follows. Using the relation (20) together with the known analytic solutions (14) and (43) we find

$$\frac{dt}{du} = \frac{2}{P_1} = \frac{2}{\sqrt{g}} = 2\sqrt{\frac{\beta^2\mu^2u^2 - 8\beta\mu u + \beta^2 + 16}{\beta u(-4\beta\mu u + \beta^2 + 16)}} = 2\sqrt{\frac{B(4B^2u^2 + 1)}{Au + 1 - 4B^2u^2}}. \quad (48)$$

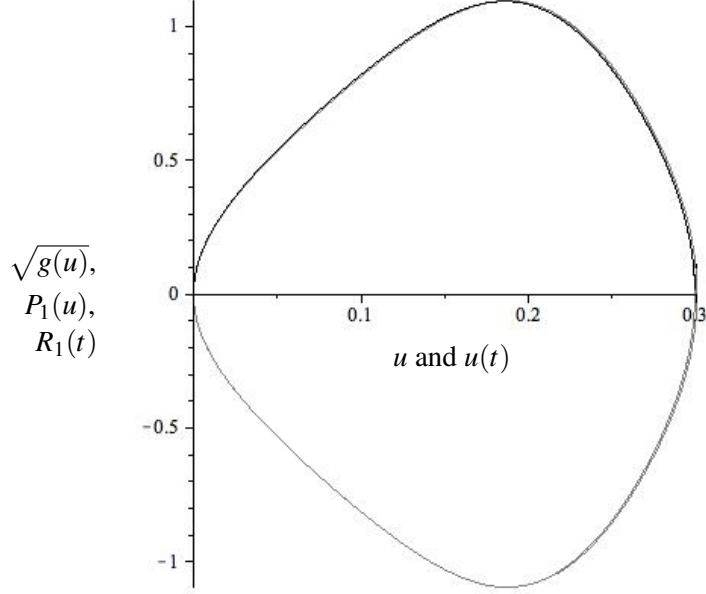


FIG. 9: Explicit matching between conventional Taub-NUT ($\sqrt{g(u)}$, dashed black), our reparameterised version of Taub-NUT ($P_1(u)$, dotted black) and the periodic vacuum DLH model mapped over using the diffeomorphism ($R_1(t)$ versus $u(t)$) as given by (15), continuous gray). They are found to lie on top of each other, with the Taub-NUT models covering the upper half plane, corresponding to the region where $g(u) \sim P_1^2(u) > 0$, whereas the DLH vacuum model winds around a closed curve in u space as it cycles through its periodic behaviour. The parameters are matched such that the periodic DLH model has the same initial conditions as considered earlier. The other radii e^ζ , P_2 and R_2 can be shown to match likewise.

This is well-defined when $g > 0$ and just recovers the positive half-period of the DLH vacuum model, as is obtained numerically (see Fig. 10). However, when $g < 0$ we can perform a Wick rotation to imaginary time $\tau = iu$. In the limit of large u where the Taub-NUT solution approaches a negative constant, we find that t and u are linearly related, but with a relative factor of i , such that $t \sim \tau \sim iu$. So the NUT regions of Taub-NUT correspond to both imaginary space and time coordinates in the DLH model. Fig. 11 displays the $u < 0$ NUT region mapped over to DLH by integrating (48) numerically. Here, we have chosen to plot the result in the first quadrant, as there is a freedom of choosing factors of $\pm i$ on both axes. At late times, the linear relationship between t and u means that this mapped NUT region also settles down to a constant like in the original Taub-NUT model. So, in particular, mapping the Taub-NUT model does not recover the periodic DLH solution, and instead corresponds to imaginary space and time. Performing the integration in (48) analytically yields a solution in terms of elliptic integrals of precisely the same form as (33),

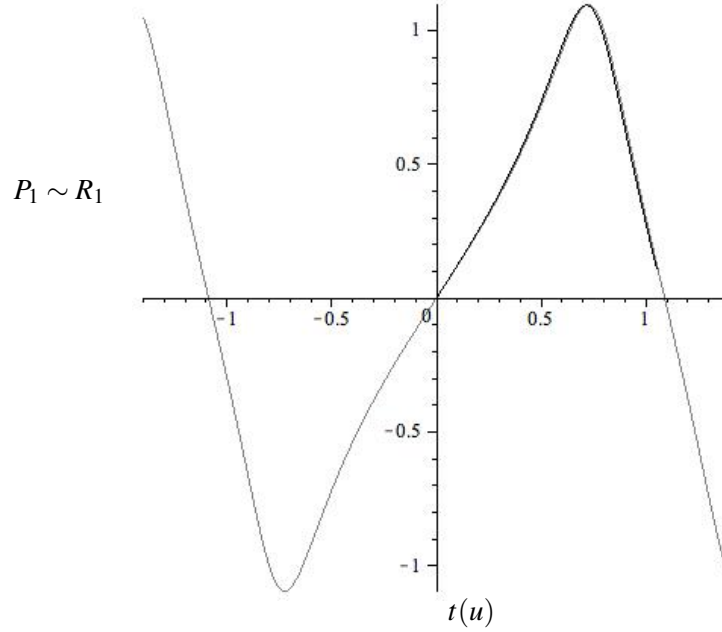


FIG. 10: The Taub region in Taub-NUT (corresponding to $g > 0$) mapped over to DLH space (black) falls on top of the the first half-period of the periodic vacuum DLH solution (grey).

as one would expect.

One marked difference between the DLH vacuum solution and this new version of the Ryan and Shepley form of the Taub-NUT solution is now that the latter is not periodic, which is the opposite of what one would commonly expect: normally Lorentzian models are not periodic, but upon euclideanising become periodic (cf. the periodicity in imaginary time of Green's and partition functions, in particular in relation to black hole thermodynamics). However, a similar phenomenon has recently also been observed in Bianchi V [33].

Note that when one allows both the positive and the negative branches of \sqrt{g} , one recovers precisely the trajectory in u - P_1 -space that the mapped DLH model traces out (Fig. 9). However, in the conventional setup Taub-NUT only selects one branch, and then turns to imaginary time and space on either side (the NUT regions, see Fig. 11). This suggests that even the Taub-NUT model could cycle indefinitely (like the vacuum DLH model) if it was allowed to change from one branch to the other. In fact, this matches smoothly: we have chosen P_1^2 to have a zero at the origin, so it is linear there from (43). Thus P_1 goes like \sqrt{u} at the origin, as also observed in Sections VII C 1 (Fig. 7) and VII D. Hence, there is actually a rather natural, smooth transition between the two branches, exactly like in Fig. 7. This also suggests that the smooth, single-valued parabolic behaviour of DLH is more natural and more fundamental, as opposed to the Taub-NUT

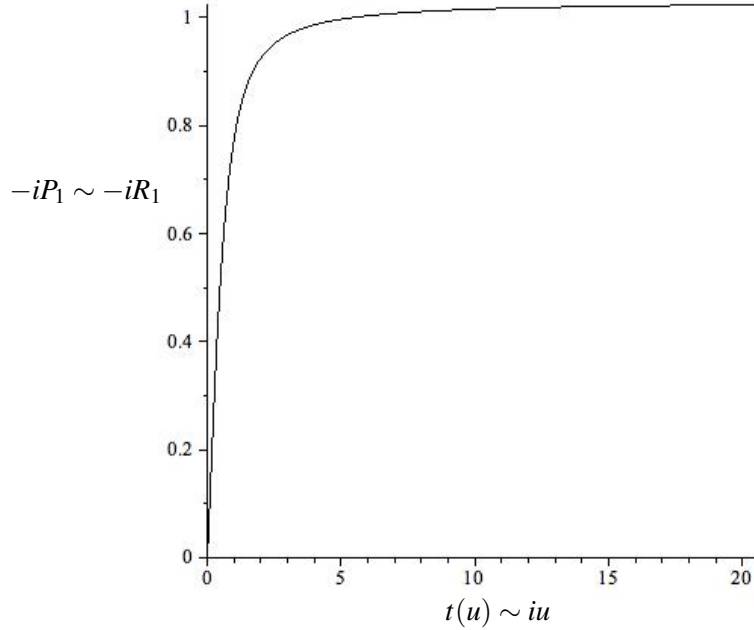


FIG. 11: First NUT region in Taub-NUT (corresponding to $u < 0$) mapped over to DLH space

case, where the parabola essentially gets turned sideways such that the description in terms of square roots results in multivaluedness by having the two different branches.

D. Taub-NUT with a scalar field

Now that we have clarified the relationship between the DLH and reparameterised Taub-NUT set-ups in the vacuum case, we can use the transformation (15) to map our cosmological DLH solution with a scalar field, presented in in [1], directly over to the reparameterised Taub-NUT model. Alternatively we could find an analogous series expansion to (22)-(24) directly.

In either case, to lowest order, the series solution has the form

$$P_1(u) = \sqrt{u}, \quad P_2(u) = \text{const}, \quad F(u) = \text{const}, \quad (49)$$

and thus analogous boundary conditions to those used in the DLH case may be used, from which a numerical integration can be performed straightforwardly.

Gradually introducing a light or diffuse scalar field has a similar effect to the analogous scenario in DLH (Section VII B), where it slightly perturbs the vacuum case. Fig. 12 shows a plot of an interesting choice of initial parameters with a sizable scalar field ($a_0 = 1.0$, $b_0 = 17$, $\kappa = 1$, $\Lambda = 0$, $f_0 = 6$, $m = \frac{1}{8}$), that exhibits inflation and isotropisation thereby looking rather like the original

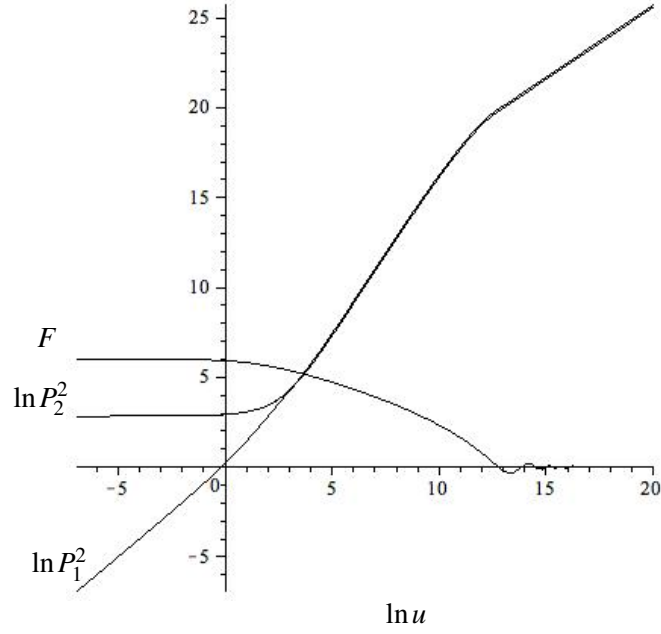


FIG. 12: Taub-NUT inflation: inflation and isotropisation in analogy to the DLH scenario for the model with parameters $a_0 = 1$, $b_0 = 17$, $\kappa = 1$, $\Lambda = 0$, $f_0 = 6$, $m = \frac{1}{8}$.

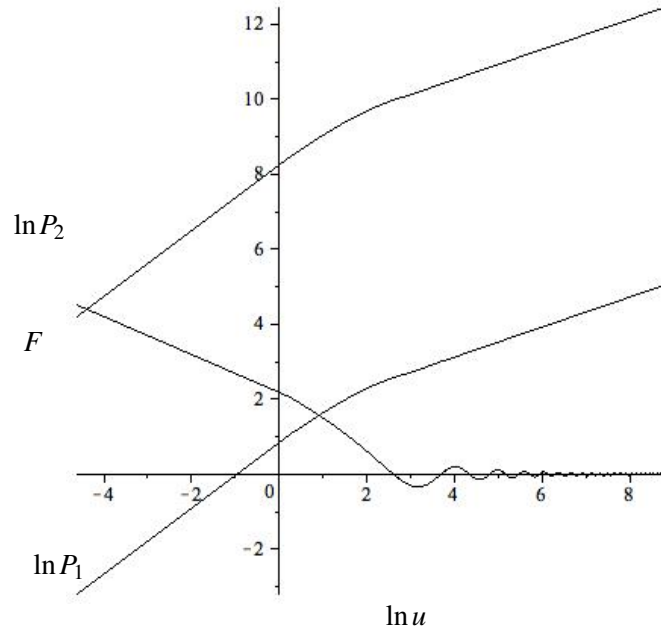


FIG. 13: Taub-NUT inflation: inflation, but not complete isotropisation for the model with parameters $a_0 = 1$, $b_0 = 2$, $\kappa = 1$, $\Lambda = 0$, $f_0 = 6$, $m = 1$.

DLH solution. Fig. 13 shows a plot of another interesting model with the set of initial parameters $a_0 = 1.0, b_0 = 2.0, \kappa = 1, \Lambda = 0, f_0 = 6, m = 1$), that exhibits inflation, but does not completely isotropise. However, the different Hubble factors tend to a common value so in the flat-space late-time limit the difference in scale factors would be unobservable as argued in [1].

The slope of P_1^2 in Fig. 12 at the pancake is unity, so that slope P_1 here is 1/2, in agreement with the DLH series solution mapped to Taub-NUT at this point (see equations (49) and (38)). The solution in Fig. 13 does not appear to be of the pancaking type, so we do not consider its early slope here. However, the late-time slopes in P_1 are 0.4 in both models (i.e. 0.8 in P_2^2). Note, that this does not agree with the behaviour $a(t) \propto t^{\frac{2}{3}}$ that one would expect once the scalar field has decayed and behaves like non-relativistic dust in an Einstein-de-Sitter phase (at which point, presumably, reheating would occur). Note, however, that the DLH model in Fig. 1 does have the required late time slope of $\frac{2}{3}$, so that the DLH coordinate time matches onto physical time at late times. So we conclude that the Taub-NUT time coordinate is not a physical time coordinate at late times, unlike the DLH time. This is consistent with the coordinate transformation (15).

We can compare the slopes in the DLH model and the corresponding Taub-NUT model for late-time power-law behaviour $R(t) = \alpha t^\beta$ as follows. The corresponding slope in Taub-NUT is

$$\frac{dP}{du} = \frac{dR}{dt} \frac{dt}{du} = \frac{dR}{dt} \frac{2}{R} = \frac{2\beta}{t}. \quad (50)$$

When we can assume that the integral in (15) is in fact dominated by the contribution from the power-law behaviour we can integrate to get

$$u = \frac{\alpha}{2(\beta+1)} t^{\beta+1} \Rightarrow t = \left(\frac{2(\beta+1)}{\alpha} u \right)^{\frac{1}{\beta+1}}. \quad (51)$$

Substituting (51) into (50) then yields

$$\frac{dP}{du} = 2\beta \left(\frac{2(\beta+1)}{\alpha} u \right)^{-\frac{1}{\beta+1}}. \quad (52)$$

Integrating we obtain

$$P(u) = \alpha^{\frac{1}{\beta+1}} (2(\beta+1))^{\frac{\beta}{\beta+1}} u^{\frac{\beta}{\beta+1}} + c. \quad (53)$$

For an Einstein-de-Sitter phase with $\beta = \frac{2}{3}$ this therefore gives $P(u) \sim u^{2/5}$, which is indeed what is observed in Figs. 12 and 13.

Fig. 14 shows $u(t)$ according to (15) in both the original DLH model with a scalar field and the new periodic vacuum solution. Note that the early time slope in $u(t)$ is 2, in agreement with

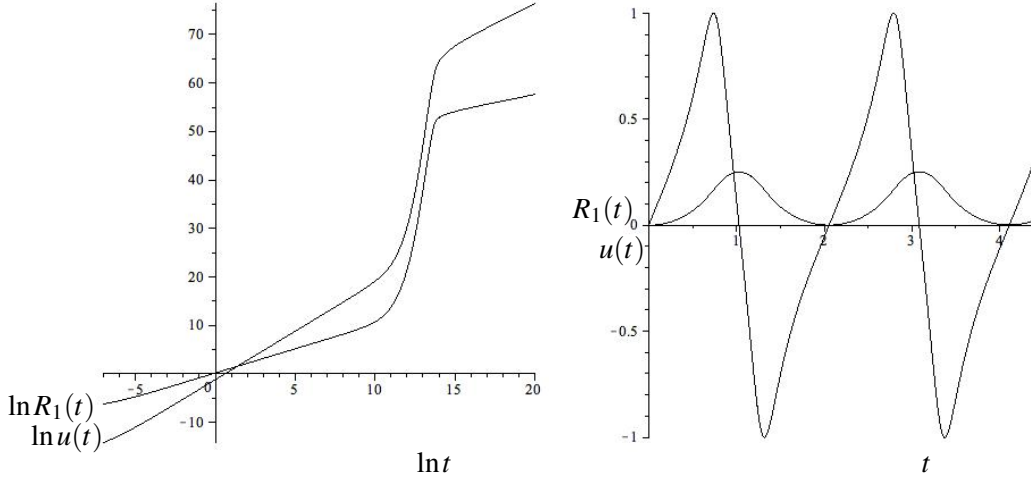


FIG. 14: $u(t)$ for the original DLH model with a scalar field (left) and the periodic vacuum DLH model (right).

formula (51) in the DLH model. The slope at late times in the DLH model is $1.67 \sim 1 + \frac{2}{3}$, also in agreement with (51). Note that the integral (15) is indeed dominated by the contribution after inflation. As already mentioned in Section V, in the periodic model $u(t)$ can be seen to go back on itself when R_1 changes sign. This means that u does not measure the progression of time in the same way as t , but instead retraces a parameter range that has been traversed previously. Considering that DLH time t matches onto physical time, this casts further strong doubts on Taub-NUT ‘time’ u being a sensible measure of time.

We conclude that the desirable features of inflation and isotropisation can survive the mapping to Taub-NUT. However, at early times – near the pancaking events – the DLH coordinatisation seems much more natural (c.f. Figs 7). At late times, the physical time coordinate can be inferred from the expansion history of the universe, and Taub-NUT again fails to match onto something physical. Furthermore the scaling solution is most natural in DLH, and very contrived in Taub-NUT coordinates. This also ties in with the fact that the closed Bianchi model is an immediate generalisation of the physical closed FRW model, which also admits such a scaling family. The multivaluedness of the Taub-NUT time coordinate when mapped from a physically meaningful model is a problem, as is allowing it to go imaginary in order to reconcile the different solutions. Thus Taub-NUT time u fails to be a physically sensible measure of time on several accounts, and we therefore contend that the DLH coordinates are the more physical coordinate system.

VIII. CONCLUSIONS

We have compared and contrasted two biaxial Bianchi IX spacetimes – Taub-NUT and the DLH model. They exhibit great similarities such as dimensional reduction at a non-singular pancaking event, inspiralling geodesics and the same eigenvalue structure of the curvature and Weyl tensors. However, there are profound differences in the global structure and physical interpretation. We have shown that the two metrics can be mapped into each other, but that the coordinate transformation is multivalued. This property is responsible for introducing artifacts into the coordinatisation and thus accounts for the differences in global behaviour. We believe that our parameterisation in terms of physical scale factors in complete analogy with, for instance, FRW-models is more natural, as opposed to working with the squares thereof and allowing those to become negative. In the light of this, we have removed the scalar field from the original DLH model and found an analytic vacuum solution in terms of elliptic integrals. This solution is periodic and also recovered by numerical integration, with which there is very good agreement. There is also an obvious link between this periodic solution and the pancaking series solution of the DLH model, in that the boundary conditions at the pancake are the same. However, after the inclusion of the scalar field the DLH model isotropised, inflated and yielded a viable late-time cosmology with a perturbation spectrum consistent with observations as shown in [1]. Thus in either case, working with the scale factors yields sensible cosmological models and, in particular, the spatial sections are closed Bianchi IX throughout, in contrast with the topology changing transition in Taub-NUT. Mapping the periodic DLH vacuum solution using the coordinate transformation matches onto the analytic Taub-NUT solution for the Taub portion where $g > 0$. However, in the NUT regions, where $g < 0$, we find that Taub-NUT time corresponds to imaginary time in ‘DLH space’. This firstly adds to the doubts that it is a sensible time coordinate; secondly, it resolves the alleged topology transition, as DLH now has closed spatial sections throughout as well as a physical time coordinate. Thirdly, and rather surprisingly, this suggests that the Lorentzian Taub-NUT is actually Euclidean in these regions. It is then surprising that the (Lorentzian) DLH model is periodic, whereas the ‘Euclidean Taub-NUT’ is not, which is contrary to what usually happens. We also note that DLH time essentially acts as conformal time for Taub-NUT.

The DLH coordinatisation thus has a number of advantages over traditional approaches. Firstly, the behaviour of the solution across pancaking events seems much more natural and straightforward in both the DLH vacuum and scalar field case. The well-behaved odd-parity series solution

that we had found previously acquired bad behaviour when mapped over to Taub-NUT due to the fact that the transformation is singular at pancaking events. Secondly, the periodicity of the DLH vacuum solution appears more fundamental than the Nut-Taub-Nut structure and in fact it is clear how this periodicity gets broken by an integral involved in the mapping. Thirdly, it is clear that the scale factor has physical significance and its square should therefore not take negative values. The resulting alternative Taub-NUT parameterisation still has the advantage of admitting a simple scaling relation over the conventional metric, which only admits a rather awkward looking scaling family. Moreover, at late times when we can infer cosmological time from physical measurements, the DLH model behaves as one would expect physically, whereas Taub-NUT time again fails to produce physical results. We conclude that our coordinatisation provides at least an interesting alternative point of view that could shed some light on some of the pathologies that Taub-NUT is believed to have, and might actually be the more natural coordinatisation.

Acknowledgments

We thank the referees for their very useful suggestions. We would also like to thank Sylvain Br chet, Nick Dorey, Gary Gibbons, Jorge Santos, Stephen Siklos, David Tong and others for helpful comments and for pointing out relevant references. PPD is grateful for support through an STFC (formerly PPARC) studentship.

Appendix A: Mapping of curvature invariants

Given the similarities in the metric Ansatz, i.e. biaxial Bianchi IX on the hypersurfaces, it was obvious that similarities between the Taub-NUT and DLH geometries should be explored. In fact, there does exist a coordinate transformation linking the two spacetimes, which we have presented above. In general, however, when one wishes to examine the relationship of two spacetimes it is often the easier strategy to show that the two spacetimes are actually distinct. This is made difficult by the general coordinate invariance of General Relativity, so one must find coordinate invariant ways to distinguish between spacetimes, such as curvature invariants. A convenient classification is the Petrov classification, which examines the algebraic properties of the Weyl tensor. This is often easier than other approaches due to the additional self-duality structure and tracelessness of the Weyl tensor (see, for instance, [34] for a reference). If, however, it turns out that the Petrov

classification is not enough to distinguish between the two spacetimes (here both are of type D) one must find more curvature invariants, such as topological invariants, or principal curvatures. If after this kind of tests one has still failed to demonstrate that the two spacetimes one wishes to compare are distinct, then the curvature invariants can be used to find the diffeomorphism linking the two spacetimes, if indeed such a diffeomorphism exists.

The Riemann and Weyl tensors $R_{\mu\nu\sigma\tau}$ and $C_{\mu\nu\sigma\tau}$ are multilinear operators of fourth rank acting on tangent vectors. However, they can also be considered as linear operators acting on bivectors, and as such they have a characteristic polynomial, whose coefficients and roots (eigenvalues) are polynomial scalar invariants. That is, consider the eigenbivector equations

$$R_{\mu\nu\sigma\tau}S^{\sigma\tau} = \lambda S_{\mu\nu}, \quad C_{\mu\nu\sigma\tau}T^{\sigma\tau} = \gamma T_{\mu\nu}, \quad (\text{A1})$$

for some bivectors $S^{\mu\nu}$ and $T^{\mu\nu}$ and eigenvalues λ and γ respectively. The degeneracy structure of the eigenvalues provides a coordinate-invariant way of distinguishing spacetimes. Consideration of the eigenbivector equation of the Weyl tensor leads to the Petrov classification, which is in general easier to examine due to the additional self-duality structure of the Weyl tensor. The eigenvalues of the Riemann tensor are also known as the ‘principal curvatures’.

1. Petrov type

There are six bivectors in $3 + 1$ dimensions, so that, in general, a fourth rank tensor acting on them has six real eigenvalues. Alternatively, the self-duality of the Weyl tensor yields a natural complex structure, so that the six real eigenvalues are equivalent to three complex eigenvalues. It turns out that both DLH and Taub-NUT have one degenerate pair of complex eigenvalues, which then also fixes the remaining one due to the tracelessness of the Weyl tensor. This corresponds to Petrov type D, which is what Taub-NUT was previously known to be. In terms of real eigenvalues, there are two degenerate pairs and two singlets. The complex structure also results in the pairs being complex conjugates of each other, and likewise for the singlets. The real eigenvalues are found to be of the form

$$\gamma_1^D = \gamma_3^D = C_1 + \sqrt{C_2}, \quad \gamma_2^D = \gamma_4^D = C_1 - \sqrt{C_2}, \quad \gamma_5^D = C_3 + \sqrt{C_4}, \quad \gamma_6^D = C_3 - \sqrt{C_4}, \quad (\text{A2})$$

for the DLH model, with some expressions C_i in terms of the R_i s and their derivatives. There is one constraint among them since the Weyl tensor is traceless, but we have suppressed the exact

results in order to avoid unnecessary clutter. Analogous results hold for the Taub-NUT model for some constants D_i , from whence the eigenvalue structure (Petrov D) and tracelessness can be seen, and the two sets of results map into each other as suggested.

Alternatively, one can consider the Weyl tensor as a function W acting on bivectors B , such that the eigenvalue equation is $W(B) = \gamma B$. The self-duality translates into $W(IB) = IW(B)$ for the complex structure denoted by I . In terms of complex eigenvalues, the eigenvalue equation becomes $W(B_i) = (\alpha_i + \beta_i I)B_i$. Solving this in the DLH and Taub-NUT setups yields the eigenvalues

$$\alpha_3^D = -2\alpha_1^D = -2\alpha_2^D, \alpha_3^T = -2\alpha_1^T = -2\alpha_2^T, \beta_3^D = -2\beta_1^D = -2\beta_2^D, \beta_3^T = -2\beta_1^T = -2\beta_2^T, \quad (\text{A3})$$

which also enjoy the appropriate degeneracy structure, mapping properties and tracelessness.

2. Principal curvatures

The Petrov classification might not be sufficient to distinguish between two spacetimes, in which case one can consider the eigenvalues of the full Riemann tensor, which are also called ‘principal curvatures’. These are more complicated, as the self-duality (and therefore natural complex structure) and tracelessness are lost. However, it again turns out that both models have two degenerate pairs of real eigenvalues, and two singlets, mirroring the structure of the Weyl tensor. Computation of the eigenvalues gives the following form

$$\lambda_1^D = \lambda_3^D = E_1 + \sqrt{E_2}, \lambda_2^D = \lambda_4^D = E_1 - \sqrt{E_2}, \lambda_5^D = E_3 + \sqrt{E_4}, \lambda_6^D = E_3 - \sqrt{E_4}, \quad (\text{A4})$$

for the DLH model, again with analogous results for the Taub-NUT case. It can be seen that these share the same degeneracy structure of the eigenvalues, which is similar to the one of the Weyl tensor. The two models can also be explicitly mapped into each other, as suggested.

Appendix B: Mapping of geodesics

In order to complete the mapping between DLH and Taub-NUT, we now turn to showing the equivalence of the geodesic equations in both models. The geodesic equations are most easily obtained using the Lagrangian formalism, in which

$$L = 4g_{\mu\nu}\dot{x}^\mu\dot{x}^\nu \quad (\text{B1})$$

is varied with respect to the coordinates $[x^\mu] = (t, x, y, z)$; here a dot denotes a derivative with respect to some affine parameter λ and the factor of 4 is included for later convenience. An explicit realisation of the Maurer-Cartan forms is, for instance,

$$\begin{aligned}\omega^1 &\equiv dx + \sin y dz, \\ \omega^2 &\equiv \cos x dy - \sin x \cos y dz, \\ \omega^3 &\equiv \sin x dy + \cos x \cos y dz.\end{aligned}\tag{B2}$$

Inserting the DLH metric (6) into L yields

$$L^D = 4\dot{t}^2 - R_1^2 \dot{x}^2 - 2R_1^2 \sin y \dot{x} \dot{z} - R_2^2 \dot{y}^2 - (R_1^2 \sin^2 y + R_2^2 \cos^2 y) \dot{z}^2.\tag{B3}$$

Since L is independent of the x - and z -coordinates, the corresponding Euler–Lagrange equations yield two conserved quantities K_x and K_z according to the relations

$$-2R_1^2 (\dot{x} + \sin y \dot{z}) \equiv K_x,\tag{B4}$$

$$-2 [R_1^2 \sin y (\dot{x} + \sin y \dot{z}) + R_2^2 \cos^2 y \dot{z}] \equiv K_z,\tag{B5}$$

which may be solved for \dot{x} and \dot{z} to yield

$$\dot{x} = \frac{K_z R_1^2 \sin y - K_x (R_1^2 \sin^2 y + R_2^2 \cos^2 y)}{2R_1^2 R_2^2 \cos^2 y},\tag{B6}$$

$$\dot{z} = \frac{K_x \sin y - K_z}{2R_2^2 \cos^2 y}.\tag{B7}$$

Substituting these expressions back into the Lagrangian, we get the modified form

$$L^D = \frac{1}{4} \frac{16\dot{t}^2 R_1^2 R_2^2 \cos^2 y - 4\dot{y}^2 R_1^2 R_2^4 \cos^2 y - (K_x^2 + K_z^2) R_1^2 + 2R_1^2 \sin y K_x K_z + K_x^2 (R_1^2 - R_2^2) \cos^2 y}{R_1^2 R_2^2 \cos^2 y}.\tag{B8}$$

The Euler–Lagrange equation for y then reads

$$4R_2^3 \cos^3 y \left(R_2 \ddot{y} + 2 \frac{\partial R_2}{\partial t} \dot{y} \right) = (K_x^2 + K_z^2) \sin y - 2K_x K_z + K_x K_z \cos^2 y,\tag{B9}$$

as stated and further analysed in [1].

For Taub-NUT we keep the same variables for now, except t is replaced by u . (In general, the 1-forms would be of the same form, but the coordinates and the affine parameter could be different.)

We will see later that this choice is indeed consistent.

$$L = 4g_{\mu\nu} \dot{x}^\mu \dot{x}^\nu\tag{B10}$$

is varied with respect to the coordinates $[x^\mu] = (u, x, y, z)$. Inserting the Taub-NUT metric in the form (17) into L yields

$$L^T = 8\dot{u}(\dot{x} + \sin y \dot{z}) - P_1^2 \dot{x}^2 - 2P_1^2 \sin y \dot{x} \dot{z} - P_2^2 \dot{y}^2 - (P_1^2 \sin^2 y + P_2^2 \cos^2 y) \dot{z}^2. \quad (\text{B11})$$

Since this Langrangian is likewise independent of the x - and z -coordinates, we still have the two conserved quantities K_x and K_z . However, they pick up an extra term in \dot{u}

$$8\dot{u} - 2P_1^2(\dot{x} + \sin y \dot{z}) \equiv K_x, \quad (\text{B12})$$

$$8\dot{u} \sin y - 2[P_1^2 \sin y(\dot{x} + \sin y \dot{z}) + P_2^2 \cos^2 y \dot{z}] \equiv K_z \equiv K_x \sin y - 2P_2^2 \cos^2 y \dot{z}, \quad (\text{B13})$$

which may be solved for \dot{x} and \dot{z} to yield

$$\dot{x} = \frac{4\dot{u}}{P_1^2} + \frac{K_z P_1^2 \sin y - K_x (P_1^2 \sin^2 y + P_2^2 \cos^2 y)}{2P_1^2 P_2^2 \cos^2 y}, \quad (\text{B14})$$

$$\dot{z} = \frac{K_x \sin y - K_z}{2P_2^2 \cos^2 y}. \quad (\text{B15})$$

Substituting these expressions back into the Lagrangian, we get the modified form

$$L^T = \frac{1}{4} \frac{64\dot{u}^2 P_2^2 \cos^2 y - 4\dot{y}^2 P_1^2 P_2^4 \cos^2 y - (K_x^2 + K_z^2) P_1^2 + 2P_1^2 \sin y K_x K_z + K_x^2 (P_1^2 - P_2^2) \cos^2 y}{P_1^2 P_2^2 \cos^2 y}, \quad (\text{B16})$$

where the terms that are linear in \dot{u} have cancelled, and the use of the conserved quantities has in fact introduced a term that is quadratic in \dot{u} .

Comparing with (B8), we see that a straightforward identification of coordinates, scale factors and affine parameters is indeed possible, and the differing terms $64\dot{u}^2 P_2^2 \cos^2 y$ and $16\dot{t}^2 R_1^2 R_2^2 \cos^2 y$ are consistent with the time rescaling (20). Therefore the equivalence of the geodesics is already exhibited at the level of the Lagrangians. The Euler-Lagrange equation for y in Taub-NUT is indeed identical to (B9), as the Lagrangians only differ on the time-time piece, which is independent of y and \dot{y} .

Appendix C: Derivation of the elliptic integral solution for the vacuum DLH model

In order to recover the analytic form of the numerical solution in Fig. 3 we note that an appropriate combination of (29) and (31) allows us to integrate a Bernoulli-type equation in $R_1(t)^{-2}$ to find R_1 in terms of R_2 and an integration constant μ as

$$R_1(t) = \pm \frac{R_2(t) \dot{R}_2(t)}{\sqrt{\mu R_2(t)^2 - 1}}. \quad (\text{C1})$$

As will become clear momentarily, we will choose the minus sign, in order to recover the analytic form of the numerical solution above. Substituting this expression for R_1 into equation (29) allows us in turn to solve for R_2 . This gives another integral solution with positive and negative branches and two integration constants. Differentiating and choosing the branch that is decreasing at $t = 0$, we lose one integration constant and can fix the other in terms of μ and b_0 such that $\dot{R}_2(0)$ vanishes in line with the pancaking series solution and the numerical solution above. From (C1), R_1 will then be increasing and vanish at $t = 0$ as asserted earlier. The slope of R_1 , which is by definition a_0 , can then be used to fix μ and hence the whole solution in terms of initial conditions

$$\mu = \frac{a_0^2 + 4}{a_0^2 b_0^2}. \quad (\text{C2})$$

With the constants in the problem explicitly fixed, we now return to the integration of R_2 and R_1 . From the denominator in (C1) this will involve finding integrals of the type

$$\sqrt{a_0^2 R_2(t)^2 + 4R_2(t)^2 - a_0^2 b_0^2} \equiv x. \quad (\text{C3})$$

In fact it can be easily seen from the numerical solution that b_0 simply scales both axes, so we set it to unity in the following. Inverting (C3) and substituting in for R_2 in terms of x gives a dynamical equation for x that can be integrated to find time t in terms of x (and thus R_2) as

$$t = \sqrt{\frac{i}{2a_0} \frac{x^2 + a_0^2}{a_0^2 + 4}} y + \sqrt{\frac{a_0}{8i}} E(y; i) + \sqrt{\frac{ia_0}{32}} (a_0 + 2i) F(y; i) - \sqrt{\frac{i}{32a_0}} (a_0^2 - 4) \Pi\left(y; \frac{2}{ia_0}; i\right), \quad (\text{C4})$$

where the elliptic integrals have been reduced in terms of Legendre's three normal forms

$$\begin{aligned} E(z; k) &= \int_0^z \frac{\sqrt{1 - k^2 s^2}}{\sqrt{1 - s^2}} ds, \\ F(z; k) &= \int_0^z \frac{1}{\sqrt{1 - s^2} \sqrt{1 - k^2 s^2}} ds, \\ \Pi(z; \nu; k) &= \int_0^z \frac{1}{(1 - \nu s^2) \sqrt{1 - s^2} \sqrt{1 - k^2 s^2}} ds. \end{aligned} \quad (\text{C5})$$

and $y \equiv \sqrt{ia_0 \frac{(x-2)}{(2x+a_0^2)}}$.

Implicit in the Legendre forms is a choice of branches. In (C4) these are chosen such that Maple's default choice indeed recovers a real solution as required. The explicit numerical evaluation of this analytic solution in Maple is confirmed to be real (to within numerical precision) and Fig. 15 shows very good agreement between the analytical solution and the results from the numerical integration for four values of a_0 : $a_0 = 0.5, 1.2, 2, 5$. Time t has been calculated as

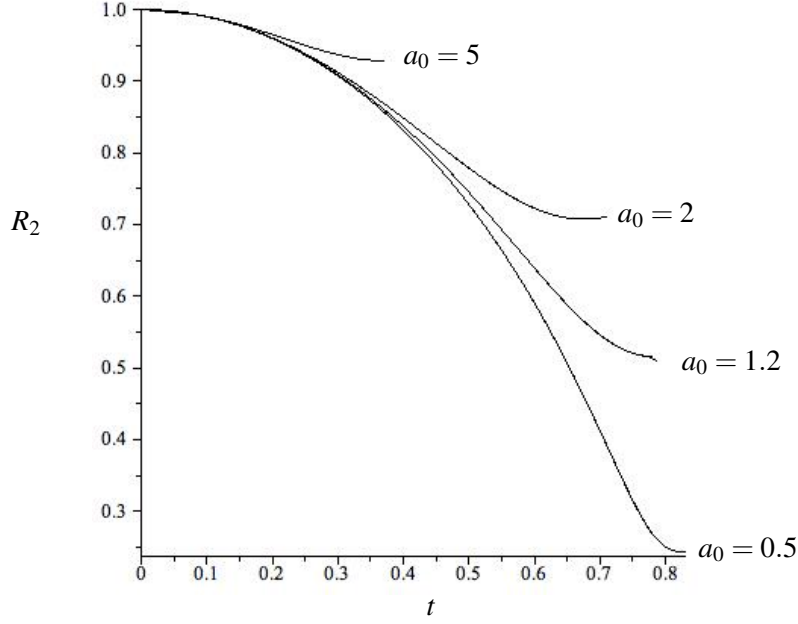


FIG. 15: Comparison of analytic and numerical solutions (which coincide) for 4 values of a_0 : $a_0 = 0.5, 1.2, 2, 5$. For each of these values the analytic expression is indeed real and coincides with the numerical result to great accuracy. Note that due to the critical factors of $\sqrt{a_0 - 2}$ in (C4) there can be relative signs depending on which branch one chooses in the function definitions as one crosses $a_0 = 2$. Here, the last two terms have flipped signs for $a_0 < 2$ when explicitly evaluated (using Maple) relative to the analytical ones in (C4). Time t is calculated as a function of R_2 in the region between the initial maximum and the first minimum of R_2 due to the multivaluedness and then plotted along the horizontal for comparison with the numerical results.

a function of R_2 between the first maximum and minimum of R_2 due to its multivaluedness, and then plotted along the horizontal axis for comparison with the numerical results.

If one repeats the above analysis for $b_0 \neq 1$ one finds that b_0 always occurs with the same power as x as might be expected from the definition. Changes in b_0 can therefore be absorbed into x . Moreover, the arguments in the elliptic functions turn out to have overall power 0 whereas the coefficients have weight one. This explains how the time t gets simply rescaled. Of course, R_2 also gets rescaled, given that b_0 is its boundary condition at $t = 0$ (which is effectively the same as

absorbing it into x).

- [1] P.-P. Dechant, A. N. Lasenby, and M. P. Hobson, *Phys. Rev. D* **79**, 043524 (2009).
- [2] L. Bianchi, *Mem. della Soc. It. delle Scienze* **11**, 267 (1898).
- [3] V. A. Belinskii, I. M. Khalatnikov, and E. M. Lifshitz, *Zh. Eksp. Teor. Fiz.* **62**, 1606 (1972).
- [4] V. A. Belinskii, I. M. Khalatnikov, and E. M. Lifshitz, *Zh. Eksp. Teor. Fiz.* **60**, 1969 (1971).
- [5] C. W. Misner, *Phys. Rev. Lett.* **22**, 1071 (1969).
- [6] I. D. Novikov and Y. B. Zel'dovich, *Annu. Rev. Astro. Astrophys.* **11**, 387 (1973).
- [7] H. Ringström, *Annales Henri Poincaré*, vol. 2, issue 3, pp. 405-500 **2**, 405 (2001).
- [8] J. M. Heinzle and C. Uggla, *Classical and Quantum Gravity* **26**, 075016 (2009), 0901.0776.
- [9] J. M. Heinzle and C. Uggla, *Classical and Quantum Gravity* **26**, 075015 (2009), 0901.0806.
- [10] M. Henneaux, *ArXiv e-prints* (2008), 0806.4670.
- [11] M. Henneaux, D. Persson, and P. Spindel, *Living Reviews in Relativity* **11**, 1 (2008), 0710.1818.
- [12] M. Henneaux, D. Persson, and D. H. Wesley, *Journal of High Energy Physics* **2008**, 052 (2008).
- [13] N. J. Cornish and J. J. Levin, in *Recent Developments in Theoretical and Experimental General Relativity, Gravitation, and Relativistic Field Theories*, edited by T. Piran and R. Ruffini (1999), pp. 616–+.
- [14] N. J. Cornish and J. J. Levin, *Phys. Rev. Lett.* **78**, 998 (1997).
- [15] N. J. Cornish and J. J. Levin, *Phys. Rev. D* **55**, 7489 (1997).
- [16] S. Calogero and J. M. Heinzle, *ArXiv e-prints* (2009), 0911.0667.
- [17] L. P. Grishchuk, A. G. Doroshkevich, and V. M. Iudin, *Zhurnal Eksperimental noi i Teoreticheskoi Fiziki* **69**, 1857 (1976).
- [18] A. Lasenby and C. Doran, *Phys. Rev. D* **71**, 063502 (2005).
- [19] M. P. Ryan and L. C. Shepley, *Homogeneous Relativistic Cosmologies* (Princeton University Press, Princeton, NJ, 1975).
- [20] D. A. Konkowski, T. M. Helliwell, and L. C. Shepley, *Phys. Rev. D* **31**, 1178 (1985).
- [21] D. A. Konkowski and T. M. Helliwell, *Phys. Rev. D* **31**, 1195 (1985).
- [22] B. Carter, Ph.D. thesis, University of Cambridge, UK (1967).
- [23] B. Carter, *Communications in Mathematical Physics* **17**, 233 (1970).
- [24] C. W. Misner and A. H. Taub, *Soviet Journal of Experimental and Theoretical Physics* **28**, 122 (1969).

- [25] S. Hawking and G. Ellis, *The Large Scale Structure of Space-Time*, Cambridge Monographs on Mathematical Physics (Cambridge University Press, Cambridge, U.K., 1973).
- [26] S. T. C. Siklos, *Communications in Mathematical Physics* **58**, 255 (1978).
- [27] V. Kagramanova, J. Kunz, E. Hackmann, and C. Laemmerzahl (2010), 1002.4342.
- [28] G. F. R. Ellis and B. G. Schmidt, *Gen. Rel. Grav.* **8**, 915 (1977).
- [29] S. Krasnikov, ArXiv e-prints (2009), 0909.4963.
- [30] D. A. Konkowski and T. M. Helliwell, in *The Tenth Marcel Grossmann Meeting. On recent developments in theoretical and experimental general relativity, gravitation and relativistic field theories*, edited by M. Novello, S. Perez Bergliaffa, and R. Ruffini (2005), pp. 1829–+.
- [31] H. Stephani et al., *Exact Solutions to Einstein's Field Equations, 2nd edition* (Cambridge University Press, 2003).
- [32] J. F. Plebański and M. Demiański, *Annals of Physics* **98**, 98 (1976).
- [33] G. Valent, *General Relativity and Gravitation* **41**, 2433 (2009), 1002.1454.
- [34] C. Doran and A. N. Lasenby, *Geometric Algebra for Physicists* (Cambridge University Press, 2003).